


Primary Open Angle Glaucoma Diagnosis Using Pattern Electroretinogram Parameters

Ahmed A Alhagaa , Nermeen Mahmoud Badawi , Osama Abd Allah El-Morsy

Ophthalmology Department, Faculty of Medicine, Menoufia University, Shebin Elkom, Menoufia, 6132415, Egypt

Correspondence: Ahmed A Alhagaa, Ophthalmology Department, Faculty of Medicine, Menoufia University, Shebin Elkom, Menoufia, 6132415, Egypt, Tel +201006742874, Fax +20482317508, Email ahmed.elhagaa@med.menofia.edu.eg

Background: Glaucoma is the most typical cause of permanent blindness. POAG, or primary open angle glaucoma, is the most common type. The pattern electroretinogram (PERG) has become a promising technique for detecting glaucoma early-on. The goal of this study was to assess the ability of PERG to diagnose POAG, especially in early, difficult-to-diagnose cases in comparison with other already established diagnostic methods.

Methods: 150 participants (300 eyes) were enrolled in a cross-sectional study at ophthalmology department at Menoufia University Hospital in August 2022 to February 2023. All recruited participants underwent comprehensive ophthalmological and PERG exams. The studied eyes were divided into three groups as 100 normal eyes (Group I), 100 eyes with preperimetric glaucoma (Group II), and 100 eyes with established perimetric glaucoma (Group III).

Results: OCT-RNFL average thickness had a significant positive correlation with P50 latency ($r=0.289$, $p=0.041$) or P50 amplitude ($r=0.302$, $p=0.018$) and N95 amplitude ($r=0.640$, $p=0.001$) among group (II). Also, RNFL thickness had negative correlation with P50 amplitude ($r=-0.268$, $p=0.043$) among group (III). RNFL thickness and P50 and N95 amplitude showed highest AUC values in detecting preperimetric glaucomatous eyes vs normal eyes (AUC=0.927, 0.952, 904), and for detecting established perimetric glaucomatous eyes vs normal eyes (AUC=1.00, 0.957, 0.983 respectively) compared with VF MD which showed AUC (0.458 and 0.901 respectively).

Conclusion: Glaucoma patients exhibit PERG alterations (comparable to RNFL thickness changes) so, it could be used as an accurate diagnostic method in POAG. Because PERG alterations occur before visual field abnormalities, it could be relied on as an early diagnostic tool in preperimetric glaucoma. We can use both RNFL thickness assessment by OCT with PERG parameters as complementary tests for accurate diagnosis of preperimetric glaucoma which represents the most difficult diagnostic challenge in glaucoma diagnosis.

Keywords: pattern electroretinogram, preperimetric glaucoma, primary open angle glaucoma, RNFL thickness

Introduction

The most common cause of lifelong blindness worldwide is glaucoma.¹ It is brought on by the death of retinal ganglion cells and the progressive degeneration of optic nerve axons.² The most prevalent type of glaucoma is primary open-angle glaucoma (POAG).³ In the absence of additional ocular or systemic anomalies, it is characterized as a set of chronic, bilateral, and asymmetric ocular illnesses in adults that cause progressive optic neuropathy (morphological changes at the retinal nerve fiber layer and optic disc) and vision field deficits.^{3,4}

Glaucoma is a leading cause of irreversible blindness worldwide and primary open-angle glaucoma (POAG) is the most prevalent clinical type of glaucoma in sub-Saharan Africa. The clinical and epidemiological profile of patients with primary open angle glaucoma often correlate with the disease.⁵ The prevalence of Primary Open Angle Glaucoma was 79.8% of all cases of glaucoma (95% CI; 68.7–84.2).⁶ One of the main factors contributing to visual impairment in glaucoma is late identification of the condition.^{7,8} As a result, to prevent irreparable harm, early detection via the development of more dependable and precise detection systems is necessary.^{9,10}

The typical abnormalities to the optic disc, the thinning of the retinal ganglion cell and nerve fiber layers, and the typical visual field deficits all point to the diagnosis of glaucoma.¹¹ Diagnosis of glaucoma at the early stages is relatively challenging due to the disparity between the start of structural and functional impairment.¹² It has been demonstrated that structural alterations in the retinal layers precede visual field abnormalities, which are caused by retinal ganglion cell (RGC) redundancy.^{10–13}

It is challenging to match axonal thinning with functional damage since the perimetric decibel scale and structural linear scale are different.^{13–16} In recent years, many researchers have attempted to directly investigate RGC function utilizing electrophysiological investigations.^{17–21} Because perimetry is dependent on patient's response to light, it is considered as a method for assessing visual function.¹⁸ Although it can identify RGC without structural axonal thinning, pattern-evoked electroretinogram (PERG) is regarded as a direct objective technique for assessing RGC function.²²

According to these findings, PERG can record the time sequences of structural loss and functional abnormalities. Because RGC dysfunction precedes RGC loss and axonal thinning, electrophysiological testing may be useful in making a diagnosis at this early stage.²³ Consequently, the purpose of this study was to assess the ability of PERG to diagnose POAG, especially in early difficult-to-diagnose cases in comparison with other already established diagnostic methods.

Subjects and Methods

Study Design and Patients

From August 2022 to February 2023, 320 eyes from 160 participants had primary open angle glaucoma (POAG) and normal subjects were enrolled. 10 subjects (20 eyes) were eliminated from the study, (3 subjects rejected consent and 7 subjects did not match the inclusion criteria); thus 150 subjects (300 eyes) agreed to participate and were included in a cross-sectional study at Menoufia University Hospitals' ophthalmology department (Figure 1). The studied eyes were divided into three groups as 100 normal eyes (Group I), 100 eyes with preperimetric glaucoma (Group II), and 100 eyes with established perimetric glaucoma (Group III).

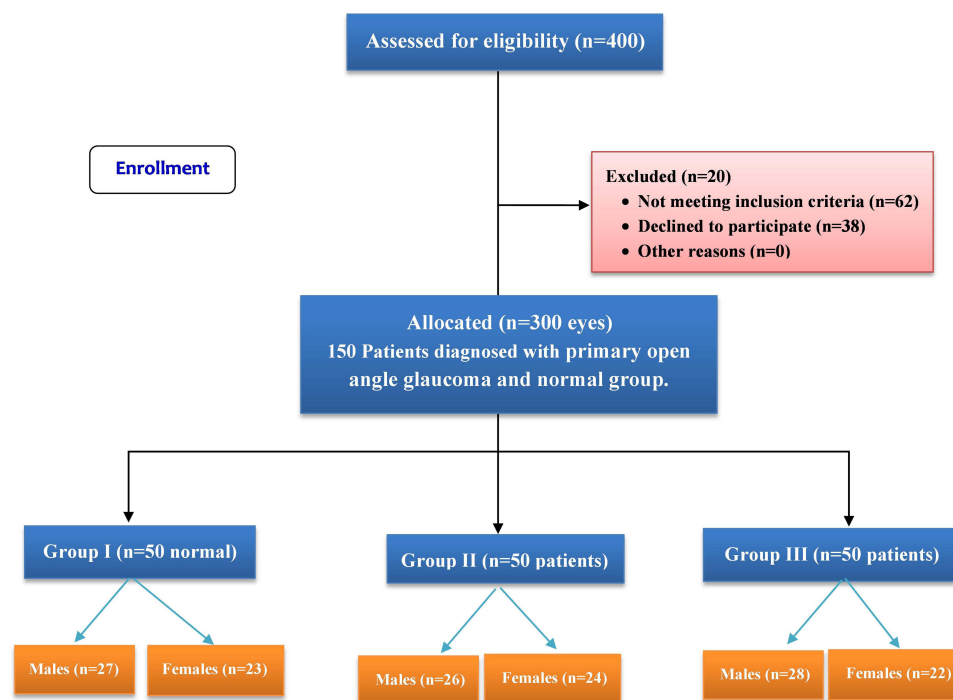


Figure 1 A flowchart of patients with primary open angle glaucoma and normal subjects.

Ethics Approval and Consent to Participate

All study protocols were designed in compliance with the Helsinki Declaration and were authorized by Menoufia University's Institutional Ethics Committee (IRB approval: 8/2022 OPHT). The patients were informed about the study's benefits, potential risks, and all stages of the procedure. Before enrolling in the study, all patients signed a written informed agreement to participate in the study.

Patients' Criteria of Our Study

Inclusion criteria: IOP < 21 mmHg, normal 24–2 Swedish interactive threshold algorithm (SITA), normal standard achromatic perimetry (SAP), and normal RNFL thickness by OCT were the inclusion criteria for healthy people (group I).

The inclusion criteria for the studied patients in this study were an open angle in gonioscopy, a glaucomatous optic nerve change associated with visual field defect in the presence of two or three of the following criteria: outside normal limits (ONL) glaucoma hemifield test (GHT), pattern standard deviation (PSD) probability less than 5%, and a cluster of three points on the pattern standard deviation probability distribution (PSD) chart.²⁴

Patients were classified as having POAG in Groups (II and III) or not having it in Group (I) based on the criteria of the *American Academy of Ophthalmology's Glaucoma, Primary Open-Angle Glaucoma Preferred Practice Pattern® Guidelines*,²⁴ which included measuring the angle of the anterior chamber, cupping the optic nerve head, having an IOP of 21 mmHg or higher, detecting visual field (VF) defects characteristic of glaucoma (in group III), and identifying optical coherence tomography (OCT) characteristic changes in groups (II and III). Patients were identified as having preperimetric glaucoma while having normal perimetric readings despite glaucoma-related OCT alterations.

Also, all patients had bilateral glaucoma, and both eyes were comparable to the degree of glaucoma.

Exclusion criteria included any systemic disease or other ocular disease other than POAG, history of head or ocular trauma, and previous ophthalmic or neurologic surgery. Progressive visual field loss in the eyes from closed-angle glaucoma, inaccurate visual field data (fixation losses > 33%, false positive and false negative > 20%), were excluded.

All Subjects Included in the Current Study Were Subjected to the Following

The thorough ophthalmological examination included visual field-testing using Humphrey Visual Field Analyzer (Humphrey Visual Field Analyzer; Carl Zeiss Meditec, Inc., Dublin, CA, USA), testing for visual acuity (VA), refraction (with and without cycloplegia), gonioscopy, intraocular pressure (IOP) measurement with a Goldmann applanation tonometer (Haag-Streit Diagnostics, Bern, Switzerland), and examination of the anterior and posterior segments.

Fixation losses, false-positive and false-negative rates, and reliability were all deemed to be less than 20% for a visual field. The pattern deviation plot was used to identify a visual field defect as three or more adjacent significant points ($p < 0.05$) and at least one of the points ($p < 0.01$) that are all situated on the same side of the horizontal meridian and are categorized as being outside of normal limits in the glaucoma hemifield test.⁶

All study participants received OCT imaging utilizing the Zeiss Cirrus HD-OCT (OCT Spectralis; Carl Zeiss Meditec AG, Germany) to measure the thickness of the RNFL in the peripapillary zone. The average RNFL thickness was taken into consideration as the primary parameter after measurements of the peripapillary RNFL thickness were taken using a 3.4-mm circular scan that was centered on the optic disc.

Anterior Chamber Angle

The anterior chamber angles were examined by gonioscopy, and diagnostic procedure. The Shaffer system gives the following description of the angle between the trabecular meshwork and the iris: Grade 4: the iris and the trabecular meshwork's surface are at a 45° angle (wide angle). Grade 3: the angle (open angle) between the iris and the trabecular meshwork surface is > 20° but less than 45°. Grade 2: 20° angle between the surface of the trabecular meshwork and the iris. Angle closure is an option. Grade 1: 10° angle between the surface of the trabecular meshwork and the iris. (Angle closure is likely to occur over time). The iris is in opposition to the trabecular meshwork, grade 0. (There is an angle closure). All study participants were grade 3.²⁴

Pattern Electroretinogram (PERG) Examinations

One qualified examiner recorded the electrophysiologic test findings using a PERG system (Metrovision, 4 rue des platanes, F59840 preches, France). Before examination, the patients were positioned in front of a display in a dimly lit room with constant background lighting of 50 lux and full optical correction in accordance with their individual refraction. On the ipsilateral side, active electrodes of the same type were implanted on the skin following the contours of the lower eyelid, and ground electrodes of 35 mm Ag/AgCl were placed on the earlobes. Silver/silver chloride skin electrodes (Technomed Europe, Maastricht, The Netherlands).

The same eyes were examined simultaneously. The visual stimulus was a checkerboard pattern with a mean brightness of 300 cd/m² and a contrast of 98% between black and white squares. The patterns on display were reversed at a rate of 4 per second when they were 60 cm away from the patients.

Intense illumination or any maneuver requiring intense illumination like fluorescein angiography was avoided before PERG recording. Each patient was requested to fixate steadily and not move his/her eyes, as ocular movements can introduce large electrical artifacts and can change electrode position which can affect results. There is no net change in luminance during the dark to light transition of the checks (the average luminance of the screen is constant over time) otherwise a luminance artifact may be introduced into the response.

The stimulus monitor screen spanned 48° of the visual field with each size of 1.8 visual angles. All participants were instructed to focus intently on the red fixation target in the monitor's center. We measured the implicit timings and P50 and N95 amplitudes. The height between N35's trough and P50's peak was utilized to determine P50's amplitude. Between the P50 peak and the N95 trough, the N95 amplitude was determined.

Statistical Analysis

For statistical analysis, IBM Corporation's Statistical Package for Social Sciences (SPSS; Armonk, New York, USA; version 25, 2022) was used. The Shapiro–Wilk test was used to determine whether the data had a normal distribution. The mean and standard deviation for quantitative data and the frequency and relative percentage for qualitative data were presented. The Chi-squared test was applied to compare the qualitative categorical data between the three groups. We used the Kruskal–Wallis test to compare more than two studied groups for quantitative variables with aberrant distribution and ANOVA *F*-test to compare more than two groups for quantitative variables with regular distribution. The visual field affection was analyzed using the visual field mean deviation (VF MD) and correlated with various PERG and peripapillary RNFL average thickness characteristics. Partial correlations were done after controlling for scan quality, refractive error, and other covariates. Statistics were considered significant for *P* values ≤ 0.05.

Results

In this study, there was no difference between the analyzed groups regarding age and sex (*P*>0.05). Also, Cup/disc ratio was substantially higher in Group (III) (0.73±0.15) than in Group (I) (0.45±0.26) and group (II) (0.51±0.30), (*P*<0.001). While mean deviation (MD) significantly decreased in Group (III) (−11.64±3.3 dB) compared to Group (I) (0.30±0.16 dB) and group (II) (0.40±0.18 dB), (*P*<0.001 for each). OCT-RNFL average thickness was considerably lower in Group (II) (71.84±5.08 μm) and group (III) (69.79±11.33 μm) than in Group (I) (117.44±11.41 μm), (*P*<0.001 for each). While the cup/disc ratio and MD did not differ among Group (I) and (II), (*P*>0.05), (Table 1).

Intraocular pressure (IOP) significantly differed among Group (I) and (II), also, among Group (I) and Group (III) (*P*<0.001). IOP was considerably significantly decreased in Group (I) (16.4±1.4 mmHg) compared to Group (II) (21.2 ±1.2 mmHg) and Group (III) (22.6±1.8 mmHg). Nevertheless, IOP did not differ among Group (II) and (III) (*p*=0.817), (data not shown in tables or figure).

Regarding PERG parameters, P50 and N95 latency were higher in Group (II) (53.43±2.62, 105.47±42.53 ms) and (III) (54.34±3.02, 108.73±30.79 ms) than in Group (I) (46.64±4.05, 90.31±3.68 ms) (*P*<0.001). However, P50 and N95 amplitude were substantially lower in Group (II) (2.52±0.43, 3.98±0.75 μV) and (III) (2.44±0.56, 3.95±0.77 μV) than in Group (I) (5.56±0.46, 7.35±0.37 μV) (*p*<0.001). Nevertheless, P50 latency and N95 did not differ among Group (II) and III (*p*>0.05), (Table 1, Figure 2A and B).

Table 1 Characteristics of Glaucoma, and Pattern Electroretinogram (PERG) Parameters Among the Studied Groups (N=300)

Variable	Group (I) (n=100)	Group (II) (n=100)	Group (III) (n=100)	Total (n=300)	F	P-value	95% CI	
							Lower	Upper
Age/Years Mean± SD Range	39.08±4.17 32–48	40.20±4.17 33–48	39.06±4.58 32–47	39.45±4.32 32–48	1.144	0.321	38.75	40.14
Sex Male Female	27 (54%) 23 (46%)	26 (52%) 24 (48%)	28 (56%) 22 (44%)	81 (54%) 69 (46%)	$\chi^2=0.161$	0.923	–	–
Cup/disc ratio Mean± SD Range	0.45±0.26 0–1.99	0.51±0.30 0–1.99	0.73±0.15 0–0.98	0.56±0.27 0–1.99	K=34.93	<0.001	0.53	0.59
Post Hoc:	P ₁ =0.39, P ₂ <0.001, P ₃ <0.001							
VF MD (dB) Mean± SD Range	0.30±0.16 0–0.9	0.40±0.18 0–1	–11.64±3.31 –14.9–(–5.2)	–3.68±5.95 –14.9–1.0	94.5	<0.001	–4.36	–3.00
Post Hoc:	P ₁ =0.081, P ₂ <0.001, P ₃ <0.001							
Average RNFL thickness (µm) Mean± SD Range	117.44±11.41 110.9–126.8	71.84±5.08 60.4–87.2	69.79±11.33 37.1–87.7	86.35±24.07 37.1–126.8	K=65.5	<0.001	83.62	89.09
Post Hoc:	P ₁ <0.001, P ₂ <0.001, P ₃ =0.250							
P50 latency (ms) Mean± SD Range	46.64±4.05 39.9–55	53.43±2.62 47.1–57.8	54.34±3.02 47.1–62.1	51.47±4.75 39.9–62.1	63.9	<0.001	50.93	52.01
Post Hoc:	P ₁ <0.001, P ₂ <0.001, P ₃ =0.28							
N95 latency (ms) Mean± SD Range	90.31±3.68 81.2–98.8	105.47±42.53 91.2–401	108.73±30.79 97.8–406.8	101.50±31.33 81.2–406.8	10.5	<0.001	97.94	105.06
Post Hoc:	P ₁ <0.001, P ₂ <0.001, P ₃ =0.16							
P50 amplitude (µV) Mean± SD Range	5.56±0.46 5–6.8	2.52±0.43 1.6–3.2	2.44±0.56 1.3–5.8	3.51±1.53 1.3–6.8	30.2	<0.001	3.34	3.68
Post Hoc:	P ₁ <0.001, P ₂ <0.001, P ₃ =0.751							
N95 amplitude (µV) Mean± SD Range	7.35±0.37 6.1–8.6	3.98±0.75 2.5–5.6	3.95±0.77 2.2–5.6	5.09±1.73 2.2–8.6	81.4	<0.001	4.89	5.29
Post Hoc:	P ₁ <0.001, P ₂ <0.001, P ₃ =0.124							

Notes: F: One way ANOVA, K: Kruskal Wallis test. P₁: Group (I) compared Group (II), P₂: Group (I) compared Group (III), P₃: Group (II) compared Group (III).
Abbreviations: OCT, optical coherence tomography; RNFL, retinal nerve fiber layer; P, positive response; N, negative response CI, confidence interval.

In this study, the VF MD did not show significant relation with RNFL thickness and PERG parameters in whole participants ($p>0.05$), (Table 2). However, among group (II), peripapillary RNFL thickness had positive correlation with P50 latency ($r=0.289$, $p=0.041$) or P50 amplitude ($r=0.302$, $p=0.018$) and N95 amplitude ($r=0.640$, $p=0.001$), (Figure 3A–C). Also, among group (III), RNFL average thickness had a significant positive correlation with P50 latency

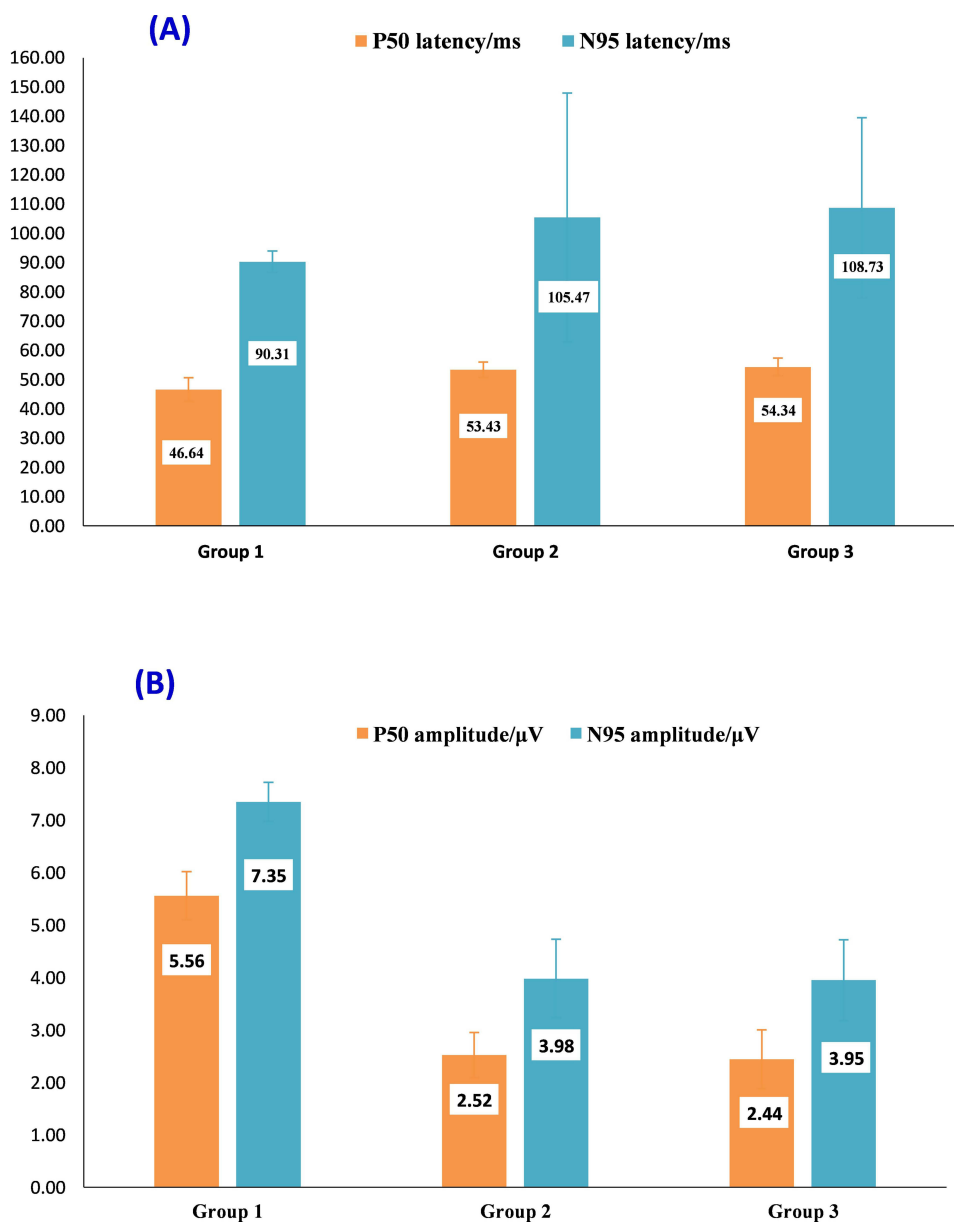


Figure 2 (A and B) PERG parameters among the studied groups.

($r=0.413$, $p=0.003$) and negative correlation with P50 amplitude ($r=-0.268$, $p=0.043$), (Figure 3D and E). While, in controls (group I) there was no substantial correlation found between OCT-RNFL thickness and PERG parameters ($P>0.05$), (Table 2).

In this study, the areas under the curve (AUCs) were 0.927, 0.952, and 0.904 for RNFL thickness and amplitude of P50 and N95, respectively in detecting preperimetric glaucomatous eyes vs normal eyes, (Figure 4A). Also, the AUCs for RNFL thickness and amplitude of P50 and N95 were 1.00, 0.957, and 0.983 respectively for detecting established perimetric glaucomatous eyes vs normal eyes (Figure 4B). The AUCs for VF MD were 0.458 and 0.901 for detecting perimetric glaucomatous and established perimetric glaucomatous eyes compared to normal eyes respectively. On the contrary, the AUC for VF MD was 0.982 for detecting preperimetric compared to established perimetric glaucomatous eyes (Figure 4C). The AUCs for RNFL thickness and amplitude of P50 and N95 were 0.582, 0.533, and 0.503 respectively, for detecting preperimetric compared to established perimetric glaucomatous eyes (Table 3).

Table 2 The Correlation Coefficient Test Between Average RNFL Thickness, PERG Parameters and VFMD in All Study Participants

	Group (I)		Group (II)		Group (III)	
	Correlation Coefficient	P value	Correlation Coefficient	P value	Correlation Coefficient	P value
Average RNFL thickness and PERG parameters in relation to VFMD						
RNFL thickness	0.037	0.800	-0.011	0.939	-0.013	0.929
P50 latency (ms)	0.179	0.213	0.038	0.793	-0.151	0.296
N95 latency (ms)	-0.084	0.564	-0.096	0.506	0.040	0.781
P50 amplitude (μ V)	0.189	0.190	-0.059	0.684	0.062	0.667
N95 amplitude (μ V)	-0.129	0.372	-0.177	0.219	0.079	0.584
Average RNFL thickness in relation to PERG parameters						
P50 latency (ms)	0.119	0.411	0.289	0.041*	0.413	0.003*
N95 latency (ms)	-0.005	0.971	0.033	0.819	-0.058	0.691
P50 amplitude (μ V)	0.083	0.567	0.302	0.018*	-0.268	0.043*
N95 amplitude (μ V)	-0.014	0.924	0.640	0.001*	0.057	0.694

Note: *Correlation is significant at the 0.01 level (2-tailed).

Abbreviations: RNFL, retinal nerve fiber layer; PERG, pattern electroretinogram; VF MD, visual field mean deviation.

Discussion

In the current study, Group (III) had a significantly higher cup/disc ratio than Group (II) and (I). In comparison to Group (II) and I, there was a substantial increase in mean deviation and quantitative assessment of RNFL by OCT in Group (I). Thickening of the nerve fiber layer and loss of vision are symptoms of glaucomatous optic neuropathy, which starts with mechanical stress in the optic disc, particularly the lamina cribrosa.²⁵⁻³⁰ Therefore, there must be a time interval between the onset of stress in the lamina cribrosa and the observable loss of retinal neurons. A previous study by Jeon et al³¹ reported that because preperimetric glaucoma refers to definite neuronal loss without perimetric degeneration, the stage is separate from preperimetric glaucoma. In clinical practice, glaucoma suspects with high C/D ratios were also considered to be functionally normal, albeit the effect of morphologic changes to the optic disc is yet unknown. In this concern, Bussel et al³² determined that RNFL remains the most important measure for glaucoma diagnosis and progression detection. Also, Moreno et al³³ found that the ganglion cell complex and peripapillary RNFL thickness were evaluated, and both showed a similar ability to distinguish healthy eyes from eyes with early glaucoma.

In the present investigation, the mean peripapillary RNFL thickness was 101.2 μ m in the normal group, 99.68 μ m in the preperimetric glaucoma group, and 74.76 μ m in the POAG group. The results are statistically significant. In the same range, North et al³⁴ found an overall mean RNFL thickness of 112.42 μ m in the normal group, 116.25 μ m in the OHT group, and 104.66 μ m in the open-angle glaucoma group.

In the present study, Groups (II) and (III) had significantly larger P50 and N95 delays than Group (I). The P50 and N95 amplitudes, however, were significantly lower in Groups (II) and (III) than in Group (I). Between Groups (II) and (III), P50 latency and N95 (latency, amplitude) did not differ substantially. In the same line, Elgohary et al²⁷ found that P50 peak time varied significantly between the GS and POAG groups, whereas N95 peak time varied significantly between the normal and POAG groups. Between the GS and POAG groups, there was a substantial difference in the PERG N95 amplitude. The prolonged P50 peak time in the normal group compared to the GS group may have been caused by the normal group's older age. Also, Porcatti et al³⁵ found that, as PERG aged, it developed a small phase lag and significantly lessened in amplitude. These results are partly in agreement with Cvenkel et al³⁶ who discovered that only the N95 amplitude can identify GS from healthy eyes, whereas both the P50 and N95 amplitudes are sensitive for early glaucoma detection. They did not, however, include P50 or N95 latency in their study. Additionally, North et al³⁴ showed that, in comparison to the control group, the P50-N95 amplitude provided slightly better discrimination between

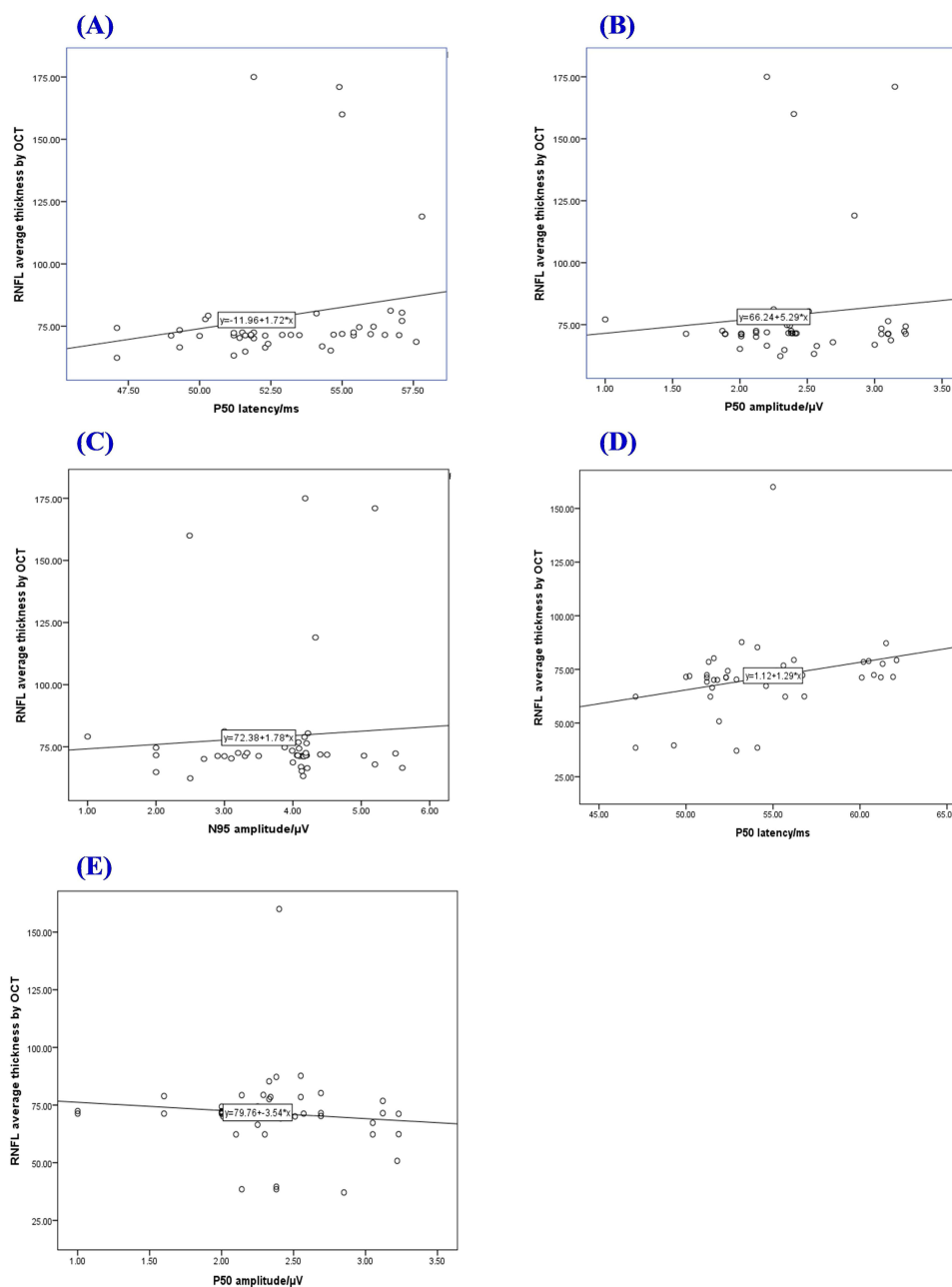


Figure 3 Correlation between average RNFL thickness and PERG parameters among the studied patients, (A–C) among group (II) and (D and E) among group (III). **Abbreviations:** RNFL, retinal nerve fiber layer; PERG, pattern electroretinogram.

the OHT and POAG groups. According to a different study by Demir et al,³⁷ the N95 amplitude was lowered more than the P50 amplitude in the POAG and OHT groups compared to the control group. Also, they found that PERG amplitude analysis could detect ganglion cell dysfunction in OHT patients before OCT or visual field problems.

The glaucomatous PERG amplitude was significantly lower than normal, in agreement with past studies.^{28,37–39} In this study, the results of time domain analysis showed a significant decrease in N95 amplitude in glaucoma eyes. However, the patient group's P50 peak's amplitude and latency in both tests did not differ noticeably. Jafarzadehpur et al³⁹ found that POAG caused a drop in the N95 amplitude but no change in amplitude or implicit time of the P50. Parisi et al⁴⁰ discovered that N95 amplitude decreased as indicated by POAG, and the PERG N95 amplitude drop in OAG eyes is a functional impairment of the deepest layers of the retina. Moreover, Ventura et al¹² reported that ganglion

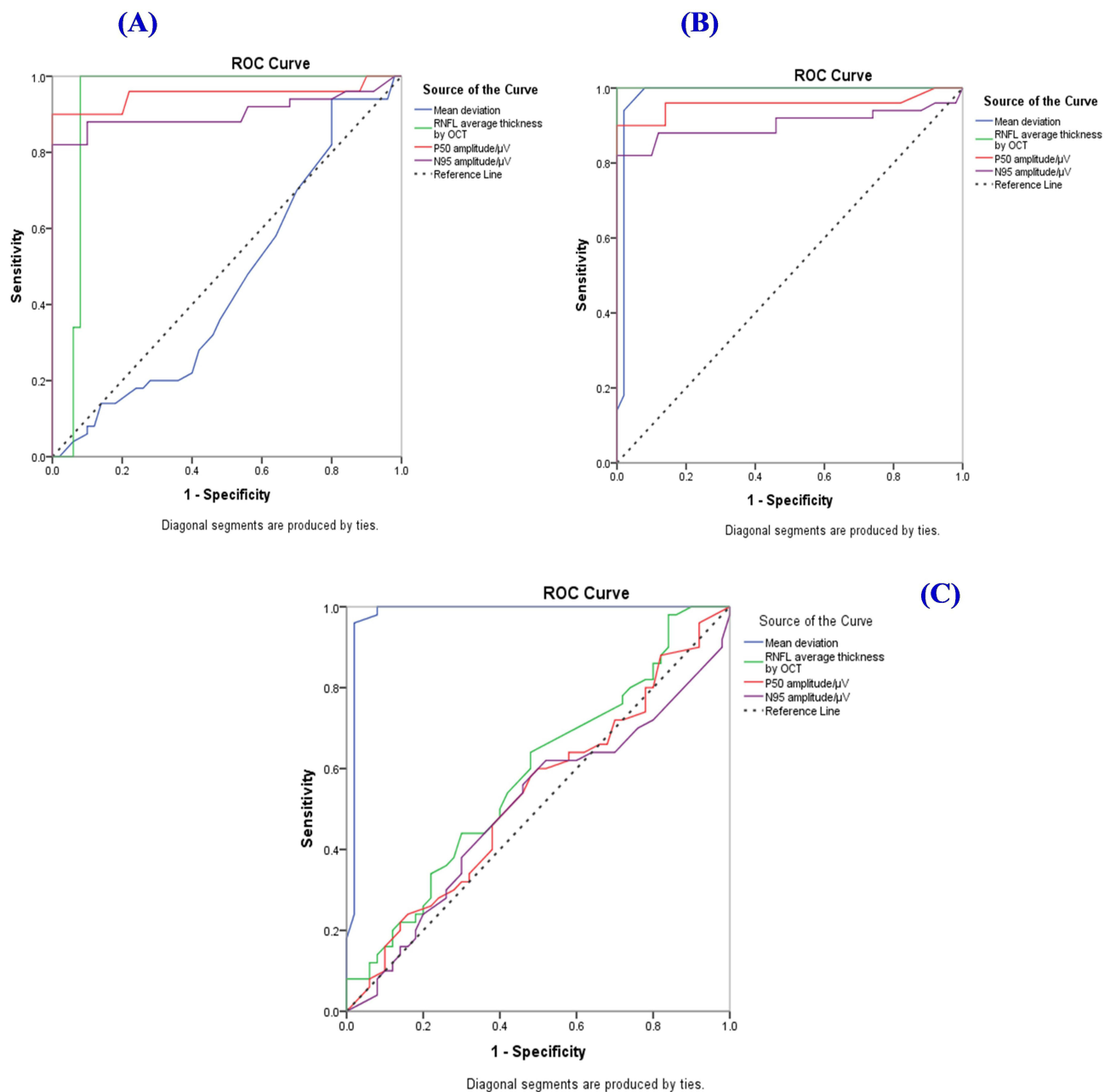


Figure 4 AUC-ROC curves of VFMD, average RNFL thickness and P50–N95 amplitude for the detection of glaucoma **(A)**, Group (I) vs Group (II) **(B)**, Group (I) vs Group (III) and **(C)** Group (II) vs Group (III).

Abbreviations: RNFL, retinal nerve fiber layer; PERG, pattern electroretinogram; POAG, primary open-angle glaucoma; VF MD, visual field mean deviation; AUC, area under curve.

cells generate N95, and by measuring its amplitude, one can infer the approximate number of ganglion cells. The severity of glaucoma relates to a drop in its amplitude.

In the current investigation, peripapillary OCT-RNFL average thickness with P50 (delay or amplitude) and N95 amplitude among group (II) showed a significant positive correlation. Additionally, among group (III), it had a significant positive correlation with P50 latency and a negative correlation with P50 amplitude. In the same line, Elgohary et al²⁷ reported peripapillary RNFL thickness significantly correlated with P50–N95 amplitude. These findings somewhat concur with those of Cvenkel et al³⁶ who discovered that only N95 amplitude could distinguish GS from healthy eyes. Similar to our investigation, the findings of the study by North et al³⁴ revealed a substantial difference in P50–N95 amplitude

Table 3 AUC Values of the VF MD and Peripapillary Average RNFL Thickness in Comparison to That of P50–N95 Amplitude for the Detection of Glaucoma

	Group I vs Group II		Group I vs Group III		Group II vs Group III	
	AUC	95% CI	AUC	95% CI	AUC	95% CI
VF MD (dB)	0.458	0.343–0.572	0.901	0.949–1.00	0.982	0.951–1.00
RNFL thickness (μm)	0.927	0.857–0.997	1.000	1.00–1.00	0.582	0.471–0.694
P50 amplitude (μV)	0.952	0.901–0.1.00	0.957	0.908–1.00	0.533	0.419–0.646
N95 amplitude (μV)	0.904	0.833–0.975	0.983	0.830–0.975	0.503	0.388–0.618

Abbreviations: RNFL, retinal nerve fiber layer; PERG, pattern electroretinogram; POAG, primary open-angle glaucoma; VF MD, visual field mean deviation; AUC, area under curve; CI, confidence interval.

between their groups. Significant correlations between N95 amplitude and RNFL thickness were found in OAG eyes by Parisi et al. The RNFL readings in these patients also closely matched the adjusted pattern standard deviation HFA.⁴¹

In the current study, most of the pERG parameters used can be described as fair tests for detection of glaucoma in comparison with the standard parameters; RNFL thickness and VF MD which showed AUC 1.00, and 0.982 respectively. In this regard, Elgohary et al.²⁷ Compared to the standard parameters, VF MD and peripapillary RNFL average thickness demonstrated AUC 0.937 and 0.846, respectively, the majority of the PERG parameters utilized in our investigation can be characterized as fair assays for the detection of glaucoma. Our results agree with Bowd et al.⁴² who reported that AUCs for the amplitude and phase of the pattern electroretinogram optimised for glaucoma screening (PERGLA) were 0.75 and 0.50, respectively. Because they can identify functional damage to the RGCs in its earliest and theoretically reversible stage, retinal electrophysiological studies, particularly PERG, are important. This advantage of PERG was proven by Guadilla et al.⁴³ in 2016 when they reported a statistically significant increase in PERG P50 and N95 amplitudes in the OHT group compared to the control group. A combination of PERG and visual evoked potential (VEP) with high and low contrast stimuli in glaucoma patients was also used by Sponsel et al.⁴⁴ North et al.³⁴ reported AUC for PERG in patients with early glaucoma was 0.787. However, the AUC value for the amplitude of P50–N90 in previous investigations on patients with early to intermediate glaucoma was 0.3435. According to Jung et al,⁴⁵ the P50–N95 amplitude in pre-perimetric glaucoma with and without RNFL abnormalities had AUC values of 0.779 and 0.618, respectively. Additionally, Kuryshva et al.⁴⁶ discovered that the amplitude of P50–N95 for early glaucoma detection and the AUC values for the full picture in face VD were 0.800 and 0.893, respectively.

Previous studies^{47–49} findings agreed with those of our study in terms of the diagnostic utility of macular VD and the amplitude of P50–N95 in patients with early glaucoma. However, their studies' results were different from ours in that the OCT-thickness and MD had a lesser diagnostic capacity than the amplitude of P50–N95. They assessed VD in a different region than we did, using a different OCTA model, and they performed ophthalmological exams after stopping topical glaucoma medication, thus their studies' findings cannot be directly compared to ours. IOP is known to have an impact on PERG responses.^{47–49} Therefore, when utilizing PERG for glaucoma evaluation, changes in IOP after stopping topical anti-glaucoma medication may be a significant complicating factor. There were some limitations of the study including small sample size and young age of patients (mean age was 39 years), thus a very young group which does not represent the general population.

Conclusion

In conclusion, glaucoma patients exhibit PERG alterations which occur early in the disease process comparable to RNFL thickness changes, so PERG could be relied on as an accurate diagnostic tool in POAG. Because PERG alterations occur before visual field abnormalities, it could be used as an early diagnostic tool in pre-perimetric glaucoma comparable to RNFL changes. In comparison to VFMD, the majority of the PERG measurements and RNFL average thickness employed in our study can be characterized as fair assays for glaucoma identification. The addition of the characteristics, such as the amplitude of P50–N95 and/or macular VD, did not significantly increase the diagnostic accuracy. Therefore, more research is required to identify the circumstances in which PERG and OCT characteristics may increase the

diagnostic accuracy for glaucoma. We can use both RNFL thickness assessment by OCT with PERG parameters as complementary tests for accurate diagnosis of preperimetric glaucoma which represents the most difficult diagnostic challenge in glaucoma diagnosis.

Abbreviations

PERG, pattern-evoked electroretinogram; POAG, Primary open-angle glaucoma; RGC, retinal ganglion cell; VF, visual field; OCT, optical coherence tomography; VA, visual acuity; IOP, intraocular pressure; SAP, standard automated perimetry; PSD, pattern standard deviation; RNFL, retinal nerve fiber layer; P, Positive response; N, negative response; ERG, electroretinogram.

Data Sharing Statement

All data and materials included in this work are available.

Author Contributions

All authors contributed significantly to the work that was published, whether it be in the ideation, study design, implementation, data collection, analysis, and interpretation, or in all these areas. They also all participated in writing, revising, or critically evaluating the article, gave their final approval for the version that would be published, agreed on the journal to which the article would be submitted, and agreed to be responsible for all aspects of the work.

Disclosure

The authors declare no competing interests in this work.

References

1. Shon K, Wollstein G, Schuman JS, Sung KR. Prediction of glaucomatous visual field progression: pointwise analysis. *Curr Eye Res.* 2014;39(7):705–710. doi:10.3109/02713683.2013.867353
2. Johnson EC, Morrison JC. Friend or foe? Resolving the impact of glial responses in glaucoma. *J Glaucoma.* 2009;18(5):341. doi:10.1097/IJG.0b013e31818c6ef6
3. Yin Z, Gao Y, Tang Y, Tian X, Zheng Y, Han Q. Aqueous humor cytokine levels are associated with the severity of visual field defects in patients with primary open-angle glaucoma. *BMC Ophthalmol.* 2023;23(1):1. doi:10.1186/s12886-023-02875-8
4. Baniyasadi N, Paschalis EI, Haghzadeh M, et al. Patterns of retinal nerve fiber layer loss in different subtypes of open angle glaucoma using spectral domain optical coherence tomography. *J Glaucoma.* 2016;25(10):865–872. doi:10.1097/IJG.0000000000000534
5. Onua AA, Awoyesuku EA, Briggs DE. Profile of primary open angle glaucoma patients attending a tertiary health institution in Niger Delta, Nigeria—a case study of 1000 patients. *J Dent Med Sci.* 2023;22(2):42–49. doi:10.9790/0853-2202024249
6. Bastola P, Bastola S, Koirala S. Prevalence, types and risk factors of glaucoma among patients attending department of ophthalmology in a tertiary care hospital: a descriptive cross-sectional study. *Med Balear.* 2023;38(5):84–88.
7. Kapetanakis VV, Chan MP, Foster PJ, Cook DG, Owen CG, Rudnicka AR. Global variations, and time trends in the prevalence of primary open angle glaucoma (POAG): a systematic review and meta-analysis. *Br J Ophthalmol.* 2016;100(1):86–93. doi:10.1136/bjophthalmol-2015-307223
8. Bettin P, Di Matteo F. Glaucoma: present challenges and future trends. *Ophthalmic Res.* 2013;50(4):197–208. doi:10.1159/000348736
9. Weinreb RN, Aung T, Medeiros FA. The pathophysiology and treatment of glaucoma: a review. *JAMA.* 2014;311(18):1901–1911. doi:10.1001/jama.2014.3192
10. Weinreb RN, Khaw PT. Primary open-angle glaucoma. *Lancet.* 2004;363(9422):1711–1720. doi:10.1016/S0140-6736(04)16257-0
11. Kreuz AC, Oyamada MK, Hatanaka M, Monteiro ML. The role of pattern-reversal electroretinography in the diagnosis of glaucoma. *Arq Bras Oftalmol.* 2014;77:403–410. doi:10.5935/0004-2749.20140101
12. Ventura LM, Sorokac N, De Los Santos R, Feuer WJ, Porciatti V. The relationship between retinal ganglion cell function and retinal nerve fiber thickness in early glaucoma. *Invest Ophthalmol Vis Sci.* 2006;47:3904–3911. doi:10.1167/iovs.06-0161
13. Medeiros FA, Zangwill LM, Bowd C, Mansouri K, Weinreb RN. The structure and function relationship in glaucoma: implications for detection of progression and measurement of rates of change. *Invest Ophthalmol Vis Sci.* 2012;53(11):6939–6946. doi:10.1167/iovs.12-10345
14. Jung KI, Park CK. Detection of functional change in preperimetric and perimetric glaucoma using 10–2 matrix perimetry. *Am J Ophthalmol.* 2017;182:35–44. doi:10.1016/j.ajo.2017.07.007
15. Rao HL, Januwada M, Hussain RS, et al. Comparing the structure–function relationship at the macula with standard automated perimetry and microperimetry. *Invest Ophthalmol Vis Sci.* 2015;56(13):8063–8068. doi:10.1167/iovs.15-17922
16. Jung Y, Park HL, Park YR, Park CK. Usefulness of 10–2 matrix frequency doubling technology perimetry for detecting central visual field defects in preperimetric glaucoma patients. *Sci Rep.* 2017;7(1):14622. doi:10.1038/s41598-017-15329-1
17. Jung Y, Park HY, Jeong HJ, Choi SY, Park CK. The ability of 10–2 short-wavelength perimetry in detecting functional loss of the macular area in preperimetric glaucoma patients. *Invest Ophthalmol Vis Sci.* 2015;56(13):7708–7714. doi:10.1167/iovs.15-17819

18. Aldebasi YH, Drasdo N, Morgan JE, North RV. S-cone, L + M-cone, and pattern, electroretinograms in ocular hypertension and glaucoma. *Vision Res.* 2004;44:2749–2756. doi:10.1016/j.visres.2004.06.015
19. Bach M, Unsoeld AS, Philippin H, et al. Pattern ERG as an early glaucoma indicator in ocular hypertension: a long-term, prospective study. *Invest Ophthalmol Vis Sci.* 2006;47(11):4881–4887. doi:10.1167/iovs.05-0875
20. Hood DC, Xu L, Thienprasiddhi P, et al. The pattern electroretinogram in glaucoma patients with confirmed visual field deficits. *Invest Ophthalmol Vis Sci.* 2005;46:2411–2418. doi:10.1167/iovs.05-0238
21. Salgarello T, Colotto A, Falsini B, et al. Correlation of pattern electroretinogram with optic disc cup shape in ocular hypertension. *Invest Ophthalmol Vis Sci.* 1999;40(9): 1989–1997.
22. Viswanathan S, Frishman LJ, Robson JG. The uniform field and pattern ERG in macaques with experimental glaucoma: removal of spiking activity. *Invest Ophthalmol Vis Sci.* 2000;41(9):2797–2810.
23. Tirsi A, Orshan D, Wong B, et al. Associations between steady-state pattern electroretinography and estimated retinal ganglion cell count in glaucoma suspects. *Doc Ophthalmol.* 2022;145(1):11–25. doi:10.1007/s10633-022-09869-9
24. Chansangpetch S, Rojanapongpun P, Lin SC. Anterior segment imaging for angle closure. *Am J Ophthalmol.* 2018;188:xvi–xxix. doi:10.1016/j.ajo.2018.01.006
25. Fiorentini A, Maffei L, Pirchio M, Spinelli D, Porciatti V. The ERG in response to alternating gratings in patients with diseases of the peripheral visual pathway. *Invest Ophthalmol Vis Sci.* 1981;21:490–493.
26. Leeman M, Kestelyn P. Glaucoma, and blood pressure. *Hypertension.* 2019;73(5):944–950. doi:10.1161/HYPERTENSIONAHA.118.11507
27. Elgohary AM, Elbedewy HA, Saad HA, Eid TM. Pattern electroretinogram changes in patients with primary open-angle glaucoma in correlation with visual field and optical coherence tomography changes. *Eur J Ophthalmol.* 2020;30(6):1362–1369. doi:10.1177/1120672119872606
28. Bode SF, Jehle T, Bach M. Pattern electroretinogram in glaucoma suspects: new findings from a longitudinal study. *Invest Ophthalmol Vis Sci.* 2011;52(7):4300–4306. doi:10.1167/iovs.10-6381
29. Quigley HA, Addicks EM, Green WR, Maumenee AE. Optic nerve damage in human glaucoma: II. The site of injury and susceptibility to damage. *Arch Ophthalmol.* 1981;99(4):635–649. doi:10.1001/archoph.1981.03930010635009
30. Meredith SP, Swift L, Eke T, Broadway DC. The acute morphologic changes that occur at the optic nerve head induced by medical reduction of intraocular pressure. *J Glaucoma.* 2007;16(6):556–561. doi:10.1097/IJG.0b013e3180575229
31. Jeon SJ, Park HY, Jung KI, Park CK. Relationship between pattern electroretinogram and optic disc morphology in glaucoma. *PLoS One.* 2019;14(11):0220992. doi:10.1371/journal.pone.0220992
32. Bussell II, Wollstein G, Schuman JS. OCT for glaucoma diagnosis, screening, and detection of glaucoma progression. *Br J Ophthalmol.* 2014;98(2):15–19. doi:10.1136/bjophthalmol-2013-304326
33. Moreno PA, Konno B, Lima VC, et al. Spectral-domain optical coherence tomography for early glaucoma assessment: analysis of macular ganglion cell complex versus peripapillary retinal nerve fiber layer. *Can J Ophthalmol.* 2011;46(6):543–547. doi:10.1016/j.cjco.2011.09.006
34. North RV, Jones AL, Drasdo N, Wild JM, Morgan JE. Electrophysiological evidence of early functional damage in glaucoma and ocular hypertension. *Invest Ophthalmol Vis Sci.* 2010;51(2):1216–1222. doi:10.1167/iovs.09-3409
35. Porciatti V, Burr DC, Morrone MC, Fiorentini A. The effects of ageing on the pattern electroretinogram and visual evoked potential in humans. *Vision Res.* 1992;32(7):1199–1209. doi:10.1016/0042-6989(92)90214-4
36. Cvenkel B, Sustar M, Perovšek D. Ganglion cell loss in early glaucoma, as assessed by photopic negative response, pattern electroretinogram, and spectral-domain optical coherence tomography. *Doc Ophthalmol.* 2017;135:17–28. doi:10.1007/s10633-017-9595-9
37. Demir ST, Oba ME, Erdoğan ET, et al. Comparison of pattern electroretinography and optical coherence tomography parameters in patients with primary open-angle glaucoma and ocular hypertension. *Turk J Ophthalmol.* 2015;45(6):229. doi:10.4274/tjo.39260
38. Bach M, Hoffmann MB. Update on the pattern electroretinogram in glaucoma. *Optom Vis Sci.* 2008;85(6):386–395. doi:10.1097/OPX.0b013e318177ebf3
39. Jafarzadehpour E, Radinmehr F, Pakravan M, Mirzajani A, Yazdani S. Pattern electroretinography in glaucoma suspects and early primary open angle glaucoma. *J Ophthalmic Vis Res.* 2013;8(3):199.
40. Parisi V, Miglior S, Manni G, Centofanti M, Bucci MG. Clinical ability of pattern electroretinograms and visual evoked potentials in detecting visual dysfunction in ocular hypertension and glaucoma. *Ophthalmology.* 2006;113(2):216–228. doi:10.1016/j.ophtha.2005.10.044
41. Parisi V, Manni G, Centofanti M, Gandolfi SA, Olzi D, Bucci MG. Correlation between optical coherence tomography, pattern electroretinogram, and visual evoked potentials in open-angle glaucoma patients. *Ophthalmology.* 2001;108(5):905–912. doi:10.1016/S0161-6420(00)00644-8
42. Bowd C, Vizzeri G, Tafreshi A, et al. Diagnostic accuracy of pattern electroretinogram optimized for glaucoma detection. *Ophthalmology.* 2009;116(3):437–444. doi:10.1016/j.ophtha.2008.10.026
43. Guadilla AM, Zaragoza P, Zato MÁ, et al. Pattern electroretinogram and ganglion cells suffering in ocular hypertensive patients. *JSM Ophthalmol.* 2016;4(2):1054.
44. Sponsel WE, Johnson SL, Trevino R, et al. Pattern electroretinography and visual evoked potentials provide clinical evidence of CNS modulation of high- and low-contrast VEP latency in glaucoma. *Transl Vis Sci Technol.* 2017;6(6):6. doi:10.1167/tvst.6.6.6
45. Jung KI, Jeon S, Shin DY, Lee J, Park CK. Pattern electroretinograms in preperimetric and perimetric glaucoma. *Am J Ophthalmol.* 2020;215:118–126. doi:10.1016/j.ajo.2020.02.008
46. Kuryshcheva NI, Maslova EV, Zolnikova IV, Fomin AV, Lagutin MB. A comparative study of structural, functional, and circulatory parameters in glaucoma diagnostics. *PLoS One.* 2018;13:e0201599. doi:10.1371/journal.pone.0201599
47. Colotto A, Salgarello T, Giudiceandrea A, et al. Pattern electroretinogram in treated ocular hypertension: a cross-sectional study after timolol maleate therapy. *Ophthalmic Res.* 1995;27:168–177. doi:10.1159/000267663
48. Ventura LM, Porciatti V, Ishida K, Feuer WJ, Parrish RK. Pattern electroretinogram abnormality and glaucoma. *Ophthalmology.* 2005;112(1):10–19. doi:10.1016/j.ophtha.2004.07.018
49. Ventura LM, Feuer WJ, Porciatti V. Progressive loss of retinal ganglion cell function is hindered with IOP-lowering treatment in early glaucoma. *Investig Ophthalmol Vis Sci.* 2012;53:659–663. doi:10.1167/iovs.11-8525

Clinical Ophthalmology

Dovepress

Publish your work in this journal

Clinical Ophthalmology is an international, peer-reviewed journal covering all subspecialties within ophthalmology. Key topics include: Optometry; Visual science; Pharmacology and drug therapy in eye diseases; Basic Sciences; Primary and Secondary eye care; Patient Safety and Quality of Care Improvements. This journal is indexed on PubMed Central and CAS, and is the official journal of The Society of Clinical Ophthalmology (SCO). The manuscript management system is completely online and includes a very quick and fair peer-review system, which is all easy to use. Visit <http://www.dovepress.com/testimonials.php> to read real quotes from published authors.

Submit your manuscript here: <https://www.dovepress.com/clinical-ophthalmology-journal>